Modeled and measured image-plane polychromatic speckle contrast

Noah R. Van Zandt
Jack E. McCrae
Steven T. Fiorino

Modeled and measured image-plane polychromatic speckle contrast

Noah R. Van Zandt,a Jack E. McCrae,a,b and Steven T. Fiorinoa,*
aAir Force Institute of Technology, Center for Directed Energy, Department of Engineering Physics, 2950 Hobson Way, Dayton, Ohio 45433, United States
bOak Ridge Institute for Science and Education, 1299 Bethel Valley Road, Oak Ridge, Tennessee 37380, United States

Abstract. The statistical properties of speckle relevant to short- to medium-range (tactical) active tracking involving polychromatic illumination are investigated. A numerical model is developed to allow rapid simulation of speckled images including the speckle contrast reduction effects of illuminator bandwidth, surface slope, and roughness, and the polarization properties of both the source and the reflection. Regarding surface slope (relative orientation of the surface normal and illumination/observation directions), Huntley's theory for speckle contrast, which employs geometrical approximations to decrease computation time, is modified to increase accuracy by incorporation of a geometrical correction factor and better treatment of roughness and polarization. The resulting model shows excellent agreement with more exact theory over a wide range. An experiment is conducted to validate both the numerical model developed here and existing theory. A diode laser source with coherence length of 259 ± 7 μm is reflected off of a silver-coated diffuse surface. Speckle data are gathered for 16 surface slope angles corresponding to speckle contrast between about 0.55 and 1. Taking the measured data as truth, both equations show error mean and standard deviation of less than 3%. Thus, the theory is validated over the range of this experiment. © *The Authors. Published by SPIE under a Creative Commons Attribution 3.0 Unported License. Distribution or reproduction of this work in whole or in part requires full attribution of the original publication, including its DOI.* [DOI: 10.1117/1.OE.55.2.024106]

Keywords: coherent optical effects; partial coherence in imaging; roughness; speckle; speckle imaging.

Paper 151373 received Sep. 30, 2015; accepted for publication Feb. 9, 2016; published online Feb. 29, 2016.

1 Introduction

In recent years, the high energy laser (HEL) community has largely shifted focus to short to medium range (tactical) mission goals such as counter-UAV (unmanned aerial vehicle) and counter-RAM (rocket, artillery, and mortar). Concurrently, there have been numerous advances in tactically relevant HEL modeling, including advances related to wave optics simulation, nonlinear thermal blooming, combined turbulence and thermal blooming effects, and lower atmosphere conditions.[1–7] However, even at shorter tactical ranges, HEL tracking requirements are very demanding.[8] Yet little published research exists regarding the potential tracking advantages of active (laser) illumination and the resulting detrimental speckle effects at tactical ranges.[9,10] Potential advantages of active illumination include eliminating dependence upon target emission and reflection of natural light, increasing signal-to-noise ratio (SNR), and increasing resolution over longer wavelength thermal imaging. However, the coherence of laser illumination also introduces detrimental speckle phenomena. Speckle causes the image of the target to break up into bright and dark patches, which degrades the ability of the tracking algorithm to estimate target position, regardless of whether that algorithm is centroid, correlation, or edge/feature based.[10,11] Thus, speckle is one source of noise in active tracking, and neglecting it can cause large inaccuracies in performance estimates. This means that speckle effects need to be well understood and characterized so that the potential advantages of active tracking can be weighed against the disadvantages of speckle.

This work investigates the statistics of tactical active-tracking speckle involving partially temporally coherent (polychromatic) illumination. The focus is on speckle contrast, C, a measure of the strength of speckle effects defined as $C = \sigma_I / \bar{I}$, where σ_I is irradiance standard deviation and $\bar{I}$ is mean irradiance. Speckle contrast is 1 for fully coherent light and 0 for completely incoherent illumination. It is reduced from unity in tactical engagements due to source bandwidth, surface slope and roughness, and the polarization properties of the reflected light. A fast and accurate numerical model for speckle contrast is developed by improving a prior engineering derivation by Huntley.[12] Improvements involve the treatment of surface roughness and polarization and the inclusion of a previously derived geometrical correction factor. The resulting modified Huntley equation matches the more exact Hu theory[13] very well over a wide range of tactically relevant conditions. An experiment is also conducted which validates both Hu and modified Huntley theory over a range of speckle contrast of about 0.55 to 1.

2 Modeling Approach

Investigation of polychromatic speckle phenomena and reduced contrast speckle began in earnest almost as early as the development of the first commercial lasers in the 1960s.[14] Polarization diversity was investigated by early researchers, often in combination with other effects.[15] The impact of surface roughness for polychromatic illumination was investigated both experimentally and theoretically in the

*Address all correspondence to: Steven T. Fiorino, E-mail: steven.fiorino@afit.edu

1970s.[16–18] Also, during that timeframe, the effects of geometry on polychromatic speckle for nonimaging systems were investigated by Pederson and Parry.[19,20] McKechnie then extended the theory to imaging systems.[21] Much later, Hu derived an expression for polychromatic speckle contrast, which allowed for any imaging and illumination geometry except those involving near glancing angles with the surface.[13] The recent work involved experimentation, extension, and engineering simplification of this theory.[12,22–25]

Three key speckle reduction factors relevant to tactical active tracking are investigated in this work, namely polarization diversity, surface roughness, and surface slope. Other factors include spatial and temporal integration. Spatial integration reduces image speckle contrast appreciably if the speckle size is comparable to or less than the pixel pitch in the detector array, as multiple speckles will influence each pixel's measurement.[14,26–28] Additionally, target motion can cause temporal decorrelation of the speckle. For example, a linearly translating target will cause time variation in the angle between the surface normal and the line of sight (LOS) of the tracker, which, in turn, causes translation of the speckle field across the aperture, along with other lesser effects. When the speckle field across the aperture decorrelates, the image speckle will also decorrelate. If the speckle changes appreciably over the integration time of the detector, speckle contrast is reduced.[15] These two factors, spatial and temporal integration, are independent of the speckle reduction factors included in the model developed here, so they can easily be added to the model. Such inclusion will not be discussed further.

The first factor considered in this work, polarization diversity, can reduce speckle contrast by up to a factor of $\sqrt{2}$.[15] Under polarized illumination, the rough surface may have the effect of separating the reflected light into two linear polarization states, each of which can produce an independent speckle field. Allowing for partial reflection degree of polarization, P_r, the speckle contrast for polarization diversity is[14]

$$C = \sqrt{(1 + P_r^2)/2}. \tag{1}$$

The second speckle reduction factor, surface roughness, also has a fairly minor impact. It reduces contrast by up to about a factor of two under realistic conditions. Under the assumptions of a Gaussian source spectrum, Gaussian surface height distribution, and no depolarization, speckle contrast for the surface reflection case is given by

$$C = \left\{ 1 + 2\pi^2 \left(\frac{\Delta\lambda}{\lambda_0} \right)^2 \left(\frac{\sigma_h}{\lambda_0} \right)^2 [\cos(\theta_{ill}) + \cos(\theta_{im})]^2 \right\}^{(-1/4)}, \tag{2}$$

where $\Delta\lambda$ is the $1/e$ full spectral width of the source, λ_0 is the mean wavelength, σ_h is the standard deviation of the surface heights, θ_{ill} is the angle between the surface normal and the incident illumination, and θ_{im} is the angle between surface normal and imaging LOS.[14] An extreme, but realistic, example might involve a wavelength of 1 μm, coherence length of 1 mm, a Gaussian spectrum, collinear illumination and imaging rays, and surface height standard deviation of 400 μm.[29] For this case, the minimum speckle contrast is 0.52 at zero slope angle, or zero angle between the imaging ray and the surface normal.

While polarization diversity and surface roughness usually reduce speckle contrast by less than a factor of two, surface slope often has a more significant impact. Hu developed a physical optics equation for speckle contrast reduction due to arbitrary illumination and imaging directions with respect to the target surface normal as

$$C^2(\theta_{im}, \theta_{ill}) = \left[1 / \int_{-\infty}^{\infty} S(\lambda) d\lambda \right]^2 \iint_{-\infty}^{\infty} d\lambda_1 \, d\lambda_2 S(\lambda_1) S(\lambda_2) \exp\{-4\pi^2\sigma^2[\cos(\theta_{im}) + \cos(\theta_{ill})]^2(1/\lambda_2 - 1/\lambda_1)^2\}$$
$$\times \frac{\left| \iint_{-\infty}^{\infty} H\left\{ \lambda_1 R\left[x - \frac{\sin(\theta_{ill})}{\lambda_1 \cos(\theta_{im})} \right], \lambda_1 Ry \right\} H^*\left\{ \lambda_2 R\left[x - \frac{\sin(\theta_{ill})}{\lambda_2 \cos(\theta_{im})} - \frac{\tan(\theta_{im})}{\lambda_1} + \frac{\tan(\theta_{im})}{\lambda_2} \right], \lambda_2 Ry \right\} dx \, dy \right|^2}{\iint_{-\infty}^{\infty} |H(\lambda_1 Rx, \lambda_1 Ry)|^2 dx \, dy \iint_{-\infty}^{\infty} |H(\lambda_2 Rx, \lambda_2 Ry)|^2 dx \, dy}, \tag{3}$$

where $S(\lambda)$ is the source spectral distribution, R is the target to aperture distance, σ is the surface height standard deviation, θ_{ill} is the angle between the surface normal and the illumination vector, θ_{im} is the angle between the surface normal and the imaging vector (with the opposite sign convention as θ_{ill}), $x = x'/\lambda R$, $y = y'/\lambda R$, x', and y' are the pupil plane spatial coordinates, and H is the pupil function.[13] Here, Gaussian distributed surface height is assumed. This equation uses few approximations, but it is not directly suitable for most real-time applications or numerical simulations of active imaging, as it requires considerable computation time due to its integral form. However, it will be taken as truth in some comparisons later on.

To address needs for a faster model of sloped surface speckle contrast, Huntley developed a simplified model for engineering applications.[12] Huntley's equation defines the number of independent coherence regions seen by each pixel based on geometrical approximations as

$$N = 1 + \frac{2r \tan(\psi + h/\rho)}{l_c}, \tag{4}$$

where $r = \sqrt{\rho^2 + h^2}$, $\rho = \alpha s$, α is a scaling constant of order unity, $s = 1.22\lambda R/D$, R is the distance between object and aperture, $h = \beta\sigma$, β is a scaling constant of order unity, σ is the surface height standard deviation, ψ is the angle between the surface normal and the bisector of the illumination and observation rays, and l_c is the source coherence length. Here, the sine function used by Huntley is replaced with a tangent function to allow accuracy to larger slope angles. In the original work, further simplifications were made which also traded accuracy

for speed. Huntley also used the common approximation for speckle contrast given N,

$$C \approx \frac{1}{\sqrt{N}}. \tag{5}$$

Further, Huntley's values for α and β were based on a curve fit of his equation to Hu's over a wide range of possible conditions.[12]

Huntley's equation is exceptionally computationally efficient, but some additional accuracy can be gained at the expense of some of that efficiency. First, speckle reduction due to roughness can be handled separately with more accuracy using Eq. (2), setting h to 0 in Eq. (4). With $h = 0$, the Huntley equation immediately reduces to

$$N = 2 \tan(\psi) \frac{\alpha \lambda R}{D l_c}, \tag{6}$$

where a factor of 1.22 has been lumped into the fitting parameter α and the leading unity term has been removed, as it is just an approximation to the geometrical corrections which will be discussed next.

Second, previously derived geometrical correction factors can be applied.[15] While these factors were derived for the one-dimensional (1-D) case of integration of speckle irradiance over time, they are still relevant to the Huntley equation. In Huntley's geometrical approximation, the N coherence areas are established as bands across the sloped target surface due to the coherence length of the illuminator separating each pixel's viewing area on target into coherence regions based on apparent surface depth (Fig. 1). When slope causes apparent depth to change by one coherence length, a new coherence region forms. Because the coherence areas are bands with long side perpendicular to the slope gradient, the problem is still 1-D, although the weight of each band is a function of the circularly approximated diffraction-limited pixel field of view. Thus, when the correction factors are applied to Huntley's N, they do not correct it perfectly. The form of the correction factor depends on the source distribution. For a Gaussian source spectrum, it is[15]
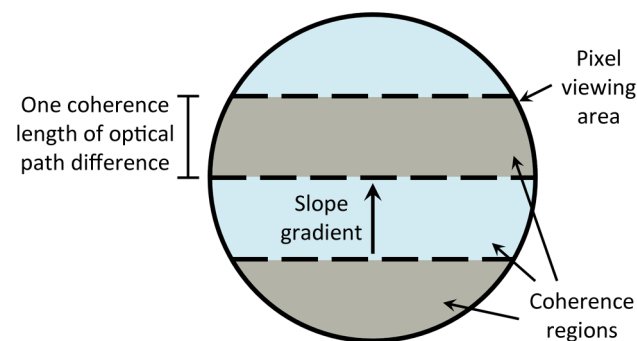
Fig. 1 A geometrically approximated circular pixel viewing area on target showing four shaded coherence zones. The zones form due to the slope of the surface and have long dimensions perpendicular to the slope gradient. Each coherence zone is separated by one coherence length of optical path difference.

$$N_{\text{eff}} = \left\{ \frac{1}{N} \text{erf}\left(\sqrt{\pi}N\right) - \frac{1}{\pi} N^{-2}[1 - \exp(-\pi N^2)] \right\}^{-1}. \tag{7}$$

For a Lorentzian distribution, it is[15]

$$N_{\text{eff}} = \left\{ \frac{1}{N} + \frac{1}{2} \frac{1}{N^2} [\exp(-2N) - 1] \right\}^{-1}. \tag{8}$$

These correction factors relate the speckle degrees of freedom from the geometrical model, N, to a corrected number of degrees of freedom, N_{eff}, which produces more accurate contrast values.

The three speckle reduction effects are then combined. This goal is accomplished through the straightforward multiplication of the numbers of degrees of freedom due to the independent reduction effects of polarization diversity and combined slope and roughness,[14] while the dependent effects of surface slope and roughness are combined in a root of the sum of the squares (RSS) fashion according to

$$N_{\text{total}} = N_{\text{P}} \left[1 + \sqrt{(N_{\text{eff}} - 1)^2 + (N_{\text{R}} - 1)^2} \right], \tag{9}$$

where N_{total} is the total speckle degrees of freedom, N_{eff} is the corrected value due to surface slope, N_{P} is due to polarization diversity, and N_{R} is due to surface roughness. N_{P} and N_{R} result from applying Eq. (5) to Eq. (1) and Eq. (2) respectively. The RSS combination of N_{eff} and N_{R} was selected from a variety of such numerically efficient combination approaches based on the least squares percent error fitting discussed next. Equation (5) is then used to compute total speckle contrast including all reduction factors.

The fitting coefficient, α, for the modified Huntley equation was found through least squares percent error fitting to Hu's theory over a wide range of tactically relevant conditions. Those conditions are shown in Table 1. They include aperture diameters of 0.3 to 1.0 m, ranges of 500 to 20,000 m, wavelengths of 1.0 or 1.5 μm, coherence lengths of 0.1 to 2.0 mm, and both Gaussian and Lorentzian source spectrums for a total of 24 fitting cases. For each case, the modified Huntley equation was fitted to Hu's theory for slopes of 0 deg to 60+ deg as shown in Fig. 2. Slope angle is the angle between the surface normal and the illumination and observation rays, which are assumed to be collinear ($\psi = \theta_{\text{ill}} = -\theta_{\text{im}}$). This assumption is typically well justified for tactical tracking when the illumination and imaging aperture separation is much less than the range to target. The overall least squares error coefficient of $\alpha = 1.749$ yielded 0.37% mean error with 2.02% standard deviation over the range of conditions tested.

Figure 2 shows a comparison of the Hu, Huntley, and modified Huntley equations under conditions for which slope dominates speckle contrast reduction. Here, the surface height standard deviation is 5 μm, a reasonable value, but one for which speckle reduction due to surface roughness is insignificant. All three models make the assumption that surface features are delta correlated spatially in the plane transverse to the surface normal. Combined with surface height standard deviation much greater than the wavelength, this surface model can be considered optically rough.[14] Hu and modified Huntley results agree well, while the original Huntley results

Table 1 Range of conditions for modified Huntley equation fitting.

| Aperture Dia. (m)	0.3	0.3	0.3	0.6	0.6	1.0	1.0	1.0	1.0	1.0	1.0	2.72 mm
Object Dist. (m)	500	500	5k	10k	20k	500	500	500	500	5k	10k	2.934
Wavelength (μm)	1.000	1.500	1.000	1.000	1.000	1.000	1.500	1.000	1.500	1.500	1.500	0.671
Coh. Lgth. (mm)	0.100	1.000	1.000	1.000	2.000	0.100	0.100	1.000	1.000	0.500	1.000	0.259
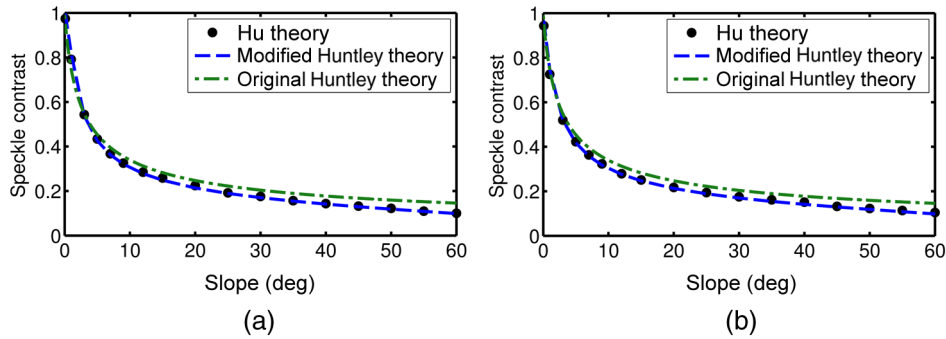
Fig. 2 Comparison of Hu, Huntley, and modified Huntley equations. (a) A Gaussian spectrum and (b) a Lorentzian. The Hu and modified Huntley equations agree well, while the original Huntley shows considerable disagreement at large slope angles. Conditions: 0.3 m aperture, 5 km range, 1 μm wavelength, 1 mm coherence length, and 5 μm surface height standard deviation.

show noticeable disagreement for the larger slope angles. The original Huntley equation was fit to Hu's theory to minimize error over a wide range of conditions, but the fit compromised large slope accuracy with tactical conditions in exchange for excellent agreement with a range of other conditions. In the modification, the inclusion of the geometrical correction factor allows small error over all slope angles.

In the previous analysis, surface roughness was not a significant factor, as is often the case for tactical active illumination. However, because Hu's theory models both slope and roughness, it is possible to compare it against both original and modified Huntley theory for conditions in which roughness is significant. Such a comparison is shown in Fig. 3. Here, both coherence length and surface height standard deviation are 1.0 mm. The illumination and imaging angles are again assumed to be collinear. The modified Huntley

equation agrees well with Hu's theory, while the original Huntley equation shows moderate error. Since both slope and roughness are significant, the geometrical correction factor still explains some of the improvement of the modified Huntley equation over the original, while the more exact treatment of surface roughness explains the rest. For 18 cases involving 30 cm aperture diameter, 5 km range, slopes of 0 deg to 60 deg, coherence lengths of 1 to 16 mm, and surface height standard deviations of 0.25 to 4 mm, the mean difference between modified Huntley and Hu was 1.98% with standard deviation of 3.33% for a Gaussian spectrum. For a Lorentzian spectrum, the mean and standard deviation of the differences were 1.36% and 2.87%, respectively. Thus, the modified Huntley equation developed here is highly accurate both when slope dominates the speckle contrast reduction (Fig. 2) and when slope and roughness both contribute to the reduction (Fig. 3).
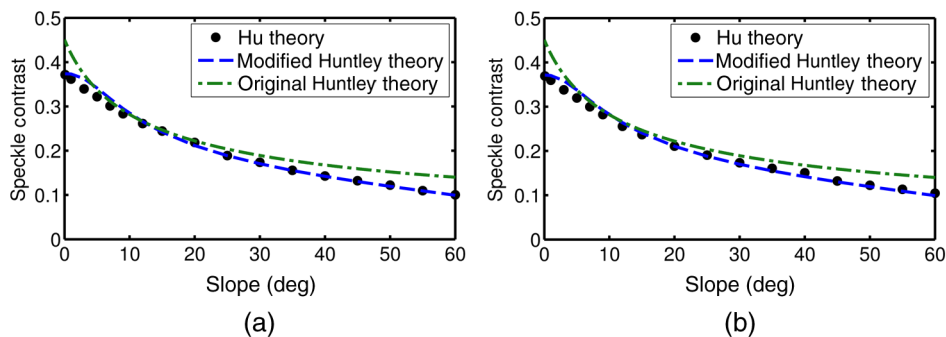
Fig. 3 Comparison of Hu, Huntley, and modified Huntley equations when both slope and roughness reduce speckle. In (a), a Gaussian spectrum is used, while a Lorentzian is used in (b). The modified Huntley matches Hu's theory very well with a region of slightly higher error for slopes between 2 deg and 10 deg. Conditions: 0.3 m aperture, 5 km range, 1 μm wavelength, 1 mm coherence length, and 1 mm surface height standard deviation.
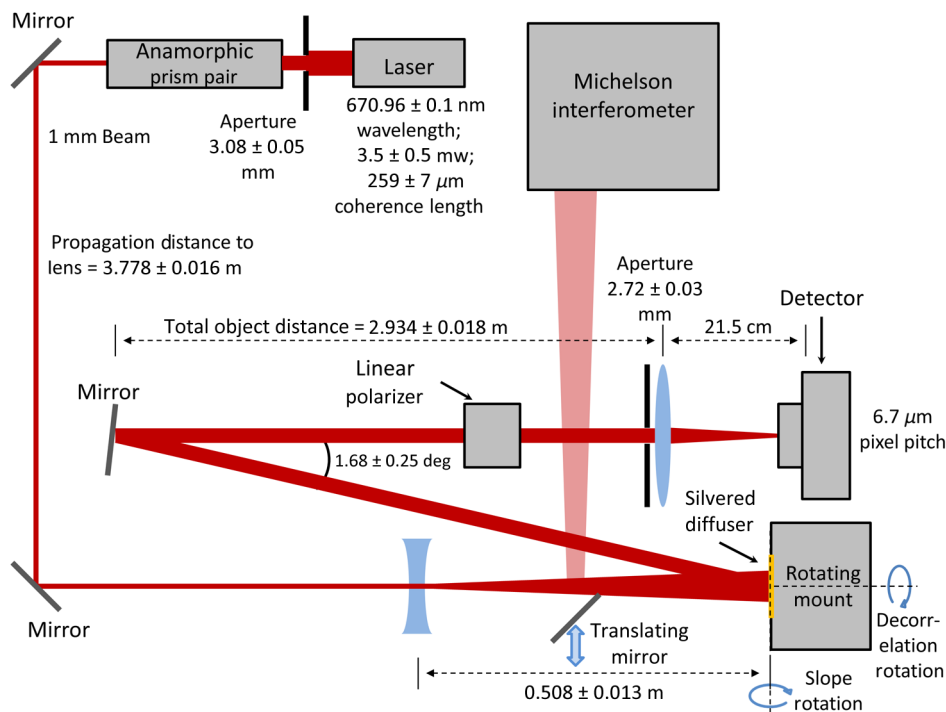
3 Experimental Validation

Hu's theory and the modified Huntley theory developed here are also validated experimentally using the layout shown in Fig. 4. A short coherence length diode laser (Toshiba T0LD9200) provides light with coherence length of $259 \pm 7~\mu$m at 56.0 mA current and 17.00°C (3.5 ± 0.5 mW output power). An aperture and prism pair reduce the elliptical beam to a 1-mm diameter circular beam, which then propagates almost 4 m and through a diverging lens to ensure coherence diameter >3 times the pixel field of view. The light scatters off of a silvered diffuser on a rotation mount for control of surface slope. Here, slope angle is the angle between the surface normal and the bisector of the illumination and imaging rays. The rotation mount both controls the slope and allows rotation of the diffuser about its surface normal, thus decorrelating the speckle between measurements and providing multiple independent speckle realizations for each slope angle. The diffuser's surface height standard deviation was measured at 3.27 μm using a profilometer, too small to impact speckle contrast. Also, the correlation length was measured at only 122 μm. These two measurements justify the surface as optically rough. The scattered light is passed through a linear polarizer to remove any effects of polarization diversity, for which Hu's theory does not allow. It is then imaged onto a focal plane for speckle measurement. The detector is a Marlin F131B complementary metal oxide semiconductor sensor with the cover glass removed to eliminate any interference effects that could otherwise arise due to reflections in the cover glass or other coatings. Alternately, the beam can be diverted to a Michelson interferometer, which allows coherence length measurement immediately prior to each speckle measurement.

The experimental dimensions represent a scaled tactical engagement. Fresnel number, $N_F = r^2/\lambda R$, where r is the aperture radius, is a common measure of diffractive conditions. For the laboratory setup, $N_F = 0.94$. For tactical tracking, reasonable dimensions are 20 km range, 30 cm aperture diameter, and 1.0 μm wavelength, which result in $N_F = 1.13$, similar to that of the lab setup. Matching speckle statistics is also desirable. For the previous conditions, coherence length of 2.0 mm, and target surface slope of 30 deg, speckle contrast is reduced to about 0.13. The experiment source power was insufficient to reach such low speckle contrast levels but did allow model validation down to about 0.55 contrast.

Figure 5 shows the measured speckle contrast compared to both Hu and Huntley theory for slope angles of 0 deg to 15 deg. The measurements have bars, which represent both vertical and horizontal error bounds. The vertical error bounds are the standard error of the mean, computed from many measurements at each slope angle and sometimes referred to as 68% confidence intervals. The width of each bar represents the uncertainty in measured slope angle. The Hu equation results are also plotted as a high and low bound representing the uncertainty in image distance and imaging aperture diameter. The figure shows excellent agreement between the measurements, Hu's theory, and the modified Huntley equation. To quantify this observation, taking Hu's theory as truth, the measurements have −1.1% mean difference with 2.9% standard deviation, while the modified Huntley equation has 1.4% mean difference with 1.0% standard deviation. The original Huntley equation also agrees well over this range, but begins to break away high around 0.55 contrast, a trend which was seen to continue in Fig. 2 due to the lack of the geometrical correction factor in this equation. From these results, both the Hu theory and the modified Huntley equation are valid models for sloped surface speckle contrast, at least over the contrast range of 0.55

Fig. 4 Validation experiment layout. A short coherence length diode laser illuminates a silvered diffuser on a rotation mount, allowing control of surface slope during speckle measurement.
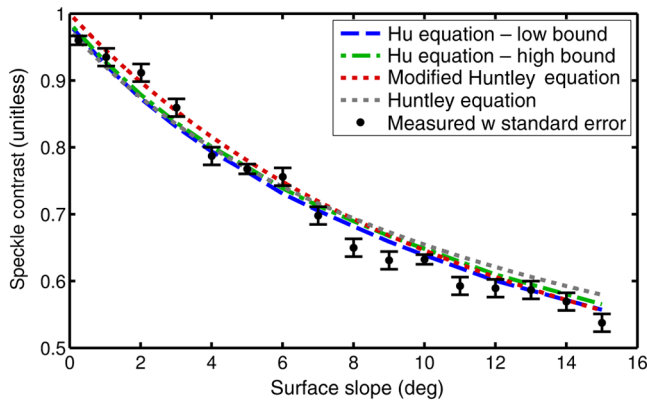
Fig. 5 Comparison of measured speckle contrast with both Hu and Huntley theory. The error bounds about the measurements are standard error of the mean, sometimes called 68% confidence intervals. Note that 11 of 16 of those error bounds encompass Hu's theory, about the expected ratio assuming Hu's theory is valid.

to 1 measured here. Unfortunately, due to lack of sufficient light, the experiment could not be extended to larger angles to more clearly separate the original Huntley equation from the others. Rather, the original Huntley equation is also found to be valid for contrast greater than about 0.7.

4 Conclusion

In this work, the statistical properties of speckle relevant to tactical active illumination were investigated with a focus on rapid numerical modeling. This focus addresses a current need in the HEL community to simulate such systems for system design, target recognition, aimpoint identification, and tracking algorithm development. The theory developed and validated here will allow understanding of both the detrimental effects of speckle as well as the possible utility of speckle for providing three-dimensional (3-D) information for identification and tracking. The later application involves the fact that speckle contrast often varies across a target due to changes in surface slope. The fast modified Huntley theory will find use in large trade studies and real-time applications for which the integral form of the Hu equation is too slow. Even so, both models were experimentally validated.

The Huntley equation for polychromatic speckle contrast, which uses geometrical approximations to reduce computation time, was improved through the incorporation of a geometrical correction factor and by independent treatment of surface roughness and polarization diversity. This modified Huntley equation was found to match the more exact Hu theory very well over a wide range of tactically relevant conditions. For 24 cases in which surface slope was the dominant speckle reduction factor, the modified Huntley equation showed mean error of 0.37% with 2.02% standard deviation. For 18 cases in which both surface roughness and slope were significant, modified Huntley showed 1.67% error with 3.12% standard deviation. Further, both the modified Huntley equation and Hu's theory were experimentally validated over a contrast range of about 0.55 to 1. For this experiment, the measurements differed from Hu by -1.1% mean and 2.9% standard deviation, while the modified Huntley disagreed by only 1.4% mean with 1.0% standard deviation. Thus, both the new modified Huntley equation and Hu's

equation are validated over the speckle contrast range of 0.55 to 1.

Areas for future research include extension of the validation range, exploitation of the 3-D information, and investigation of the impact of optical turbulence. First, the SNR issues which prevented measurements below about 0.55 speckle contrast could be overcome to extend the model validation range either by implementing further noise suppression or using a source capable of maintaining very short coherence length at higher output power. Further, because speckle contrast varies with surface slope, it carries 3-D target information. Exploitation of that information could prove useful for target identification, aimpoint identification, or aimpoint tracking. Finally, because tactical illumination involves light propagation through the turbulent atmosphere, the effects of optical turbulence on polychromatic illumination speckle contrast should be investigated.

References

1. R. A. Motes, S. A. Shakir, and R. W. Berdine, "An efficient scalar, non-paraxial beam propagation method," *J. Lightwave Technol.* **30**(1), 4–8 (2012).
2. B. G. Ward, "Modeling of transient modal instability in fiber amplifiers," *Opt. Express* **21**(10), 12053–12067 (2013).
3. A. M. Ngwele and M. R. Whiteley, "Scaling law modeling of thermal blooming in wave optics," Technical Report NGIT ABL A&AS, MZA Associates Corporation, Dayton, Ohio (2006).
4. J. D. Barchers, "Linear analysis of thermal blooming compensation instabilities in laser propagation," *J. Opt. Soc. Am. A* **26**(7), 1638–1653 (2009).
5. N. R. Van Zandt, S. T. Fiorino, and K. J. Keefer, "Enhanced fast-running scaling law model of thermal blooming and turbulence effects on high energy laser propagation," *Opt. Express* **21**(12), 14789–14798 (2013).
6. S. T. Fiorino et al., "Effectiveness assessment of tactical laser engagement scenarios in the lower atmosphere," *J. Aero. Info. Systems* **10**(1), 32–39 (2013).
7. S. T. Fiorino et al., "Climate change: anticipated effects on high-energy laser weapon systems in maritime environments," *J. Appl. Meteor. Climatol.* **50**, 153–166 (2011).
8. N. R. Van Zandt et al., "Comparison of coherent and incoherent laser beam combination for tactical engagements," *Opt. Eng.* **51**(10), 104301 (2012).
9. R. Baribeau and M. Rioux, "Influence of speckle on laser range finders," *Appl. Opt.* **30**(20), 2873–2878 (1991).
10. J. F. Riker, "Requirements on active (laser) tracking and imaging from a technology perspective," *Proc. SPIE* **8052**, 805202 (2011).
11. R. Baribeau and M. Rioux, "Centroid fluctuations of speckled targets," *Appl. Opt.* **30**(26), 3752–3755 (1991).
12. J. M. Huntley, "Simple model for image-plane polychromatic speckle contrast," *Appl. Opt.* **38**(11), 2212–2215 (1999).
13. Y. Hu, "Dependence of polychromatic-speckle-pattern contrast on imaging and illumination directions," *Appl. Opt.* **33**(13), 2707–2714 (1994).

14. J. W. Goodman, *Speckle Phenomena in Optics: Theory and Applications*, Roberts & Company, Englewood, CO (2007).
15. J. W. Goodman, *Statistical Optics*, John Wiley & Sons, Inc., New York (2000).
16. R. A. Sprague, "Surface roughness measurement using white light speckle," *Appl. Opt.* **11**(12), 2811–2816 (1972).
17. H. M. Pederson, "On the contrast of polychromatic speckle patterns and its dependence on surface roughness," *Opt. Acta: Int. J. Opt.* **22**(1), 15–24 (1975).
18. K. Nakagawa and T. Asakura, "Average contrast of white-light image speckle patterns," *Opt. Acta: Int. J. Opt.* **26**(8), 951–960 (1979).
19. H. M. Pederson, "Second-order statistics of light diffracted from Gaussian, rough surfaces with applications to the roughness dependence of speckle," *Opt. Acta: Int. J. Opt.* **22**(6), 523–535 (1975).
20. G. Parry, *Laser Speckle and Related Phenomena*, Springer-Verlag, Berlin (1975), Chapter 3.
21. T. S. McKechnie, "Image-plane speckle in partially coherent illumination," *Opt. Quantum Electron.* **8**, 61–67 (1976).
22. C. M. P. Rodrigues and J. L. Pinto, "Contrast of polychromatic speckle patterns and its dependence to surface heights distribution," *Opt. Eng.* **42**(6), 1699–1703 (2003).
23. I. Markhvida et al., "Influence of geometry on polychromatic speckle contrast," *J. Opt. Soc. Am. A* **24**(1), 93–97 (2007).
24. L. Tchvialeva et al., "Using a zone model to incorporate the influence of geometry on polychromatic speckle contrast," *Opt. Eng.* **47**(7), 074201 (2008).
25. L. Tchvialeva, I. Markhvida, and T. K. Lee, "Error analysis for polychromatic speckle contrast measurements," *Opt. Lasers Eng.* **49**, 1397–1401 (2011).
26. J. Bures, C. Delisle, and A. Zardecki, "Détermination de la Surface de Cohérence à Partir d'une Expérience de Photocomptage," *Can. J. Phys.* **50**(8), 760–768 (1972).
27. J. W. Goodman, *Laser Speckle and Related Phenomena*, Springer-Verlag, Berlin (1975), Chapter 2.
28. T. S. McKechnie, *Laser Speckle and Related Phenomena*, Springer-Verlag, Berlin (1975), Chapter 4.
29. B. Stanton, W. Coburn, and T. J. Pizzillo, "Armor plate surface roughness measurements," ARL-TR-3498, Army Research Laboratory, Adelphi, Maryland (2005), www.dtic.mil/cgi-bin/GetTRDoc?AD=ADA432918.

Noah R. Van Zandt is a PhD student with the Center for Directed Energy at the Air Force Institute of Technology (AFIT) in Dayton, Ohio. He received his BS degree in electrical engineering from Cedarville University in 2010 and his MS degree in optical science and engineering from AFIT in 2015. His research interests include atmospheric propagation of high energy lasers, laser beam combination, and active and passive target tracking. He is a student member of SPIE.

Jack E. McCrae received his PhD in physics from the AFIT in 1997, an MS in physics (optics) AFIT in 1993, and a BS degree in physics from the MIT in 1984. He is a retired Air Force colonel and currently a research assistant professor in the Engineering Physics Department at AFIT. His research interests include optics, lasers, quantum and non-linear optics, laser radar, atmospheric propagation, and imaging.

Steven T. Fiorino received his BS degree in geography and meteorology from Ohio State (1987) and Florida State (1989) Universities, respectively. He additionally holds an MS degree in atmospheric dynamics from Ohio State (1993) and a PhD in physical meteorology from Florida State (2002). He is an AFIT research associate professor of atmospheric physics with research interests in microwave remote sensing, weather signal processing algorithms, and atmospheric effects on military weapon systems. He is a member of SPIE.